Purdue University
Purdue e-Pubs

CTRC Research Publications | Cooling Technologies Research Center

1-1-2022

Investigation of Thermal Properties and Thermal Reliability of Ga-based Low Melting Temperature Alloys as Thermal Interface Materials (TIMs)

Y. Wu

R. Kantharaj

A. Alsaati

A. M. Marconnet

C. Handwerker

Follow this and additional works at: https://docs.lib.purdue.edu/coolingpubs

Wu, Y.; Kantharaj, R.; Alsaati, A.; Marconnet, A. M.; and Handwerker, C., "Investigation of Thermal Properties and Thermal Reliability of Ga-based Low Melting Temperature Alloys as Thermal Interface Materials (TIMs)" (2022). *CTRC Research Publications.* Paper 421.
http://dx.doi.org/https://doi.org/10.1007/978-3-030-92381-5_132

This document has been made available through Purdue e-Pubs, a service of the Purdue University Libraries. Please contact epubs@purdue.edu for additional information.

Investigation of Thermal Properties and Thermal Reliability of Ga-based Low Melting Temperature Alloys as Thermal Interface Materials (TIMs)

Yifan Wu, Rajath Kantharaj, Albraa Alsaati, Amy Marconnet, and Carol Handwerker

Abstract Gallium-based low melting temperature alloys have been proposed as candidates for next generation thermal interface materials (TIMs) due to their high thermal conductivity (~30 W/m*K) and liquidity. However, poor wettability as well as embrittling and corroding effect of Ga on metals have limited their use by the electronics industry. Studies on the relationship between the evolution of thermal properties and interfacial reactions between Ga-based TIMs and metal substrates are thus vital for creating a path forward. We measured thermal conductivity and thermal interface resistance of eutectic Ga-In alloy (EGaIn) sandwiched between two Ni-plated Cu substrates following simulated assembly and accelerated aging. The rapid interfacial reaction between EGaIn and both Ni and Cu at elevated temperatures led to an increase in the thermal conductivity. Further study showed the change in thermal properties was due to the depletion of Ga in the system through intermetallic formation, creating a higher conductivity In-rich alloy.

Keywords Ga alloys · Low melting temperature alloys (LTAs) · Thermal interface materials (TIMs)

Introduction

For electronic devices, heat dissipation is becoming increasingly challenging as a result of both the increase in power density and the decrease in dimensions of products. Effective thermal management is thus critical to the design and development of electronic devices. One aspect of thermal management is the use of thermal interface materials (TIMs) at interfaces between different components to reduce thermal contact resistance and temperature rises in the system. Thermal contact resistance arises from the inevitable surface roughness of mating surfaces. At a solid–solid interface, apart from a few point-point contacts, most of the interfacial volume is occupied by air, which is a poor conductor of heat. Thermal interface materials

---

Y. Wu · R. Kantharaj · A. Alsaati · A. Marconnet · C. Handwerker (✉)
Purdue University, West Lafayette, IN, USA
e-mail: caroh@purdue.edu

© The Minerals, Metals & Materials Society 2022

TMS 2022 151st Annual Meeting & Exhibition Supplemental Proceedings,
The Minerals, Metals & Materials Series,
https://doi.org/10.1007/978-3-030-92381-5_132

improve heat conduction across interfaces by filling in the air gap and reducing the thermal interface resistances. An ideal thermal interface material has high thermal conductivity, high conformability, and good wetting with the target surfaces, as well as being nontoxic and environmentally friendly.

The most extensively used TIMs are thermal greases which combinations of silicone and thermally conductive particle fillers [1]. Due to the intrinsically low conductivity of silicone, the thermal conductivity of even high-performance thermal greases is generally less than 10 W/m K [2]. Gallium-based low melting temperature alloys have recently emerged as candidates for next generation TIMs due to several factors. First, Ga offers a high thermal conductivity of 30 W/m K [3] and a relatively low melting temperature (for a metal) of only 29.8 °C. Further, unlike its near-room temperature liquid metal counterparts, Ga is unique in the way that it is not radioactive (like Rb), explosively reactive (like Fr and Cs), nor toxic (like Hg). By alloying Ga with other elements (*e.g.*, In, Sn, or Zn), a melting temperature well below room temperature can be easily achieved. For instance, the eutectic Ga-In alloy (EGaIn with 24.5 wt.% In) has a melting temperature of 15.5 °C, and the commercial product Galinstan (an alloy of Ga, In, and Sn) has a reported melting temperature of −19 °C [4]. In addition to its low melting temperature, Ga and its alloys are known experience significant undercooling due to the difficulty in nucleation upon cooling, making it possible for Ga-based alloys to maintain its liquid state for an extended temperature range. As a low viscosity liquid, Ga-based alloys can easily flow in the air gaps formed at solid–solid interfaces, offering improved heat flow [5]. Furthermore, in stark contrast to mercury, the most commonly used room temperature liquid metal, Ga, has a very low vapor pressure (10^{-12} mmHg) [6], making the dry-out issue commonly found in TIMs less of a concern for Ga and its alloys.

Despite all these advantages, the wetting behavior and reactivity with other metals have prevented Ga-based low melting temperature alloys from being widely adopted as TIMs in commercial products. In terms of wettability, pure Ga is a high surface tension metal. The surface tension of liquid gallium is 0.707 N/m [7], which means Ga simply does not wet most metal surfaces. Furthermore, Ga is highly susceptible to oxidation and rapidly forms an oxide layer (Ga_2O_3) when exposed to oxygen, which lowers its surface energy [6]. The low viscosity, high surface tension liquid and its elastic, and high adhesion oxide result in a viscoelastic behavior of Ga-based liquid metals. This complicates their wetting behavior in oxygen-containing environments. The high reactivity of Ga with other metals also presents a challenge. On certain metal substrates, for example Al, Ga wets the grain boundaries and percolates the entire structure causing subsequent structural failure, known as liquid metal embrittlement [8]. On metals like Cu, Ga forms intermetallic compounds (IMCs) rapidly with the solid metal substrate [9]. Since these metals are used extensively in the electronic industry, reaction between Ga and them can lead to premature failure of the device and thus must be mitigated.

Considerable work has been done on Ga-based liquid metal alloys, most of which target the wettability issue. Because of the low surface tension and high adhesion offered by the naturally formed Ga_2O_3, a lot of the work tackling the poor wettability of Ga center themselves around the manipulation of the oxide layer [10].

A common and intuitive method is to incorporate high thermal conductivity solid particle fillers into Ga-based alloys to alter the rheology of the liquid metal [11–17]. Tang et al. [11] synthesized a series of $CuGa_2$-EGaIn amalgams by doping copper particles into EGaIn matrix with different packaging ratios with the $CuGa_2$ particles forming as a reaction product between Ga and Cu. With increasing packing fractions, the amalgams showed a liquid-like to paste-like transition, an increase in thermal conductivity, and improved wetting on metal surfaces. Similar studies based on the principle of incorporating solid metal particles into Ga-based liquid metal matrices via intermetallic compound formation can also be found in Ga-Ag and Ga-Mg systems [12, 13]. Similar liquid metal-solid particle pastes were also achieved using an oxide-mediated method rather than an IMC formation route in Ga-W, Ga-Diamond, and Ga-quartz systems [14–16]. Alternatively, Gao et al. [17] devised a method of micro-oxidation to improve wetting by increasing the percentage of Ga_2O_3 in the liquid metal matrix through stirring in an oxygen-containing environment. Despite its simplicity, this method suffers from the low thermal conductivity due to the oxide. Instead of modifying the Ga-based liquid metal itself, researchers have also explored the potential of using Ga-based alloys in liquid metal-polymer composites [12, 18, 19]. Although the end products show lower thermal conductivity compared to liquid metal itself, this method has the advantages of preventing leakage of the liquid metal while greatly improve the thermal conductivity of the polymer composite. For example, Tutika et al. [19] achieved a thermal conductivity of 11 W/m K by dispersing EGaIn in a silicone elastomer.

Most previous studies on liquid metal TIMs have focused on addressing the wettability issue while preserving or improving the thermal conductivity. However, little work has been done to quantify the thermal performance of such materials in contact with metal substrates. Therefore, in this study, we created Cu-LM-Cu joints using an oxide-mediated spontaneous wetting technique. The thermal performance of the Ga-based alloy as a TIM on a Ni-coated Cu substrate was investigated as a function of thermal history, including aging at 125 °C. The microstructural evolution of the TIM and the substrate due to interfacial reactions, intermetallic formation, and corrosion has been related to changes in thermal properties and composition of the liquid metal. The thermodynamics aspect of Ga-based alloys was also discussed to facilitate the understanding of interfacial reactions and the resulting thermal properties.

Experimental

Materials and Sample Preparation

The liquid metal eutectic Ga-In (EGaIn) was prepared by combining 75.5 wt.% Ga and 24.5 wt. In (Rotometal). Ni-coated (5 microns, electroplated) Cu substrates were cut into 10 mm × 10 mm pieces and used as the metal substrate to sandwich the liquid metal TIM, as shown in Fig. 1. To facilitate wetting, a layer of Ga_2O_3 was deposited

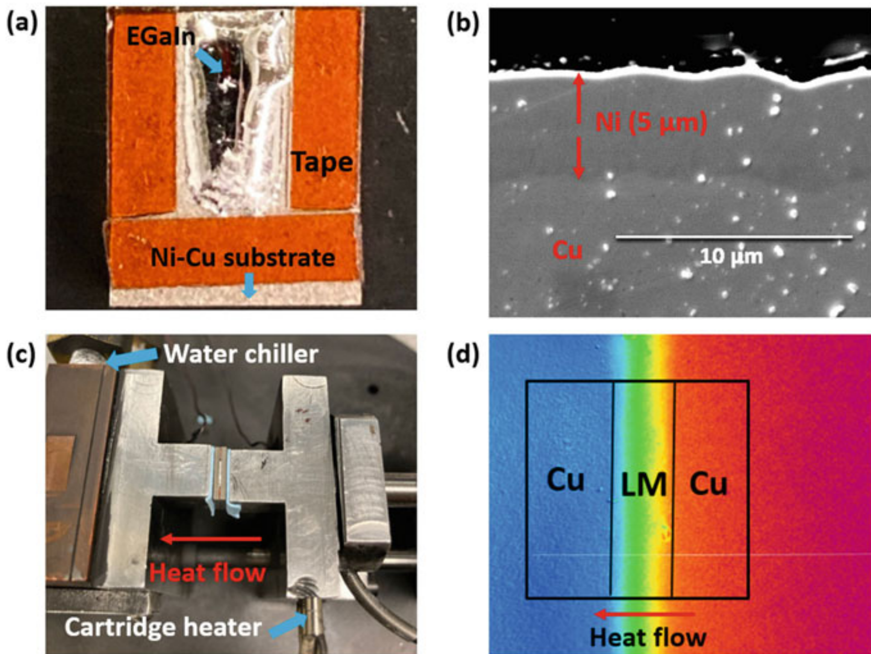

Fig. 1 **a** Image of one of the 2 sides of a Cu-LM-Cu joint illustrating the EGaIn within a pocket created on the Ni-coated Cu substrate with double-sided tape; **b** SEM image of the cross-section of the Ni-plated Cu substrate; **c** overview of the IR temperature mapping setup; **d** example temperature map of a Cu-LM-Cu joint with the different regions for analysis outlined

on the surface by scrubbing a small droplet of EGaIn with a cotton swab prior to the application of the bulk liquid. Accelerated aging was carried out to study the effect of processing and thermal aging on the stability of the interface. To mimic the reflow process during assembly, several specimens were reflowed in a DDM Novastar GF-12HC-HT 3-zone reflow oven for one and five cycles using a reflow profile for SAC solders, which has a peak temperature of 260 °C. For thermal aging, specimens were annealed at 125 °C for various amounts of time (0 day, 5 days, 10 days, and 15 days) in a Fisher Scientific 725F annealing furnace. A commercial TIM, ARCTIC APT 2560 Thermal Pad, was also tested for comparison.

Thermal Testing and Microstructural Characterization

Two specimens that underwent the same thermal treatment were joined together using heat resistant tapes, exposing one edge for IR temperature imaging using a QFI InfraScope MWIR Temperature Mapping Microscope. Calculations of thermal conductivity and thermal interface resistance were based on the principles based on

the ASTM D-5470 standard adapted for use with infrared thermal mapping [20, 21]. In this setup, the Cu-LM-Cu joint was sandwiched between two aluminum bars. During measurements, the aluminum bar with cartridge heaters served as the heat source, while the one connected to a fixed temperature water chiller served as the heat sink, as shown in Fig. 1. The top of the sample was lightly sprayed with graphite to increase its emissivity. A total of four temperature maps with different heat flux were taken for each sample by changing the power output of the cartridge heater.

At each power level, the sample was allowed to reach steady state prior to recording the temperature profile. For analysis, a 1D temperature profile along the heat flow direction was calculated from each 2D map by averaging the temperature normal to the heat flow direction (each column in the image in Fig. 1d). Assuming 1D heat transfer and minimal losses, the heat flux was constant through each layer and across the interfaces. Thus, by measuring the slope in temperature of each layer and the temperature jump at interfaces, the thermal conductivity and thermal interface resistance of the Ga alloy TIM was measured based on:

$$q^{'} = -k_1 \left.\frac{dT}{dx}\right|_1 = -k_{ref} \left.\frac{dT}{dx}\right|_{ref} = \frac{\Delta T_{int}}{R_{int}} \quad (1)$$

where $q^{''}$ is the heat flux through the sample stack, k_1 is the thermal conductivity of the TIM, k_{ref} is the thermal conductivity of the reference material, ΔT_{int} is the temperature jump at the interface, and R_{int} is the thermal contact resistance (in m^2 K/W). In this study, Cu was the reference material, thus k_{ref} has a value of 386 W/m K.

After IR imaging, samples were taken apart. Excess liquid metal was brushed off for differential scanning calorimetry (DSC) testing using Thermal Analysis Q2000 in copper pans. The substrates were then rinsed with 5% HCl solutions to remove as much LM as possible to reveal interfacial reaction products. The interfacial reaction products were imaged using SEM (Quanta 650). Energy-dispersive spectroscopy (EDS) analysis was performed to identify intermetallic phases formed.

Results and Discussion

Thermal Properties

Figure 2 shows the evolution of the thermal conductivity with annealing and reflow. The EGaIn prior to any aging had a thermal conductivity of 29.9 W/m K, in good agreement with existing literature. During annealing at 125 °C, it shows an initial decrease in thermal conductivity after 5 days of aging. However, the thermal conductivity dramatically increased to 37.6 W/m K after 10 days of aging. After 15 days, the thermal conductivity decreased to 32.7 W/m K, which is still higher than its original

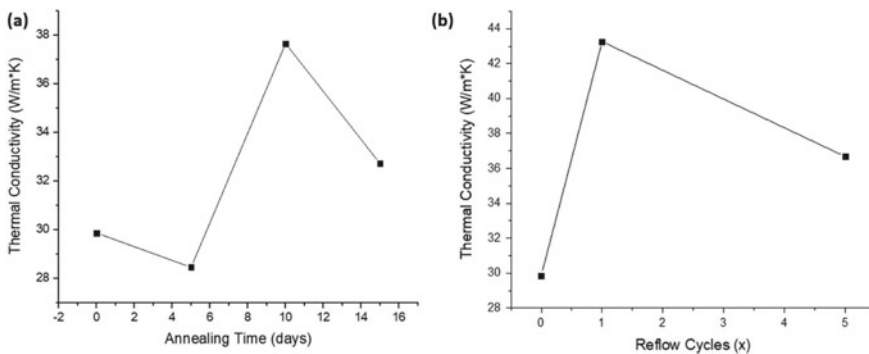

Fig. 2 Thermal conductivity of Ga-based TIMs after **a** annealing at 125 °C and **b** reflow

value. Changes in thermal conductivity as a function of reflow cycles show a similar trend. After one cycle of reflow using a SAC alloy reflow profile, the thermal conductivity of the TIM in the joint increased to 43.3 W/m K but decreased to 36.7 W/m K upon further reflow.

One advantage of using liquid metal as TIM is the high conformability it offers and henceforth the low thermal boundary resistance. As shown in Fig. 3, prior to aging, the EGaIn-Cu interface is measured to have a remarkably low thermal boundary resistance of 3.4×10^{-8} m^2K/W. In comparison, the ARCTIC APT2560 thermal pad's thermal boundary resistance was measured to be 2.2×10^{-7} m^2K/W, which is an order of magnitude higher than that of the liquid metal. After 5 days of annealing at 125 °C, the thermal boundary resistance slightly increased to 3.5×10^{-8} m^2K/W, before decreasing to 2.8×10^{-8} m^2K/W after 10 days. The thermal boundary resistance after 15 days of annealing showed a slight increase from the 10 days sample but still remained lower than the original value. A similar trend is also seen in reflowed samples.

The increase in thermal conductivity and decrease in thermal boundary resistance suggest an improved thermal performance of EGaIn after accelerated aging on Ni-Cu

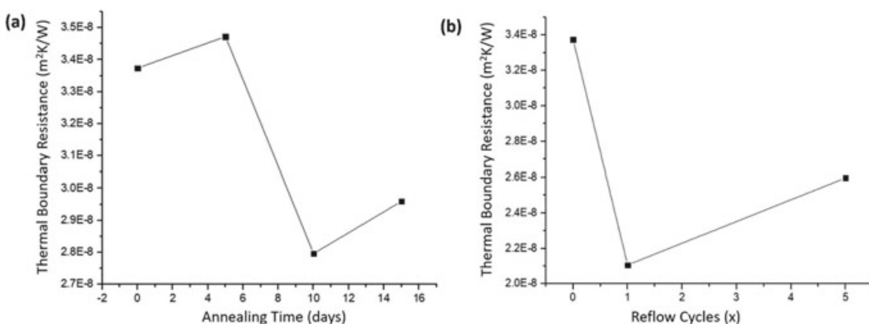

Fig. 3 Thermal boundary resistance of Ga-based TIMs after (a) annealing at 125 °C and (b) reflow

substrates. This is counterintuitive as generally a decrease in thermal performance would be expected from an interface that is deteriorating as the interfacial reaction takes place. One possible explanation for this observation could be the change in alloy composition as a result of rapid interfacial reaction at elevated temperatures, as discussed in Sect. "Interfacial Reaction Products".

Interfacial Reaction Products

The EGaIn/Ni-Cu interface after annealing at 125 °C and reflow is shown in Fig. 4. After annealing for 5 days, intermetallic compound $(Ni,Cu)_3Ga_7$ formed as a result of

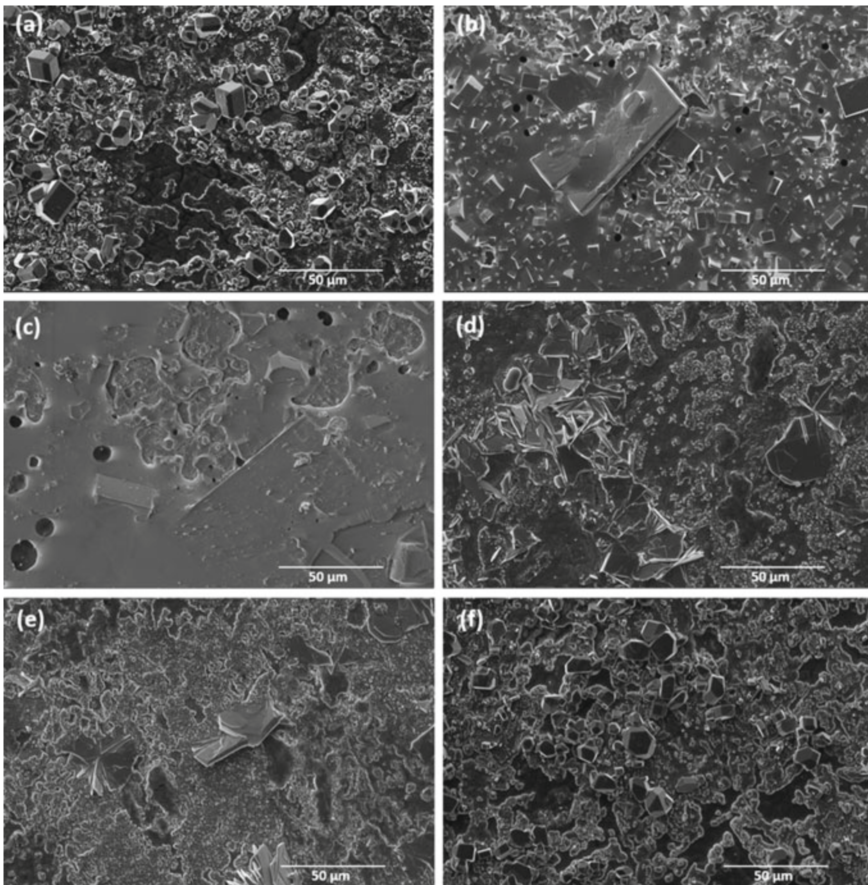

Fig. 4 EGaIn/Ni-Cu interface with EGaIn partially removed to reveal reaction products after **a** 5 days annealing at 125 °C; **b** 10 days annealing at 125 °C; **c** 15 days annealing at 125 °C; **d** 1 × reflow;e 5 × reflow; and **f** 5 × reflow + 5 days annealing at 125 °C

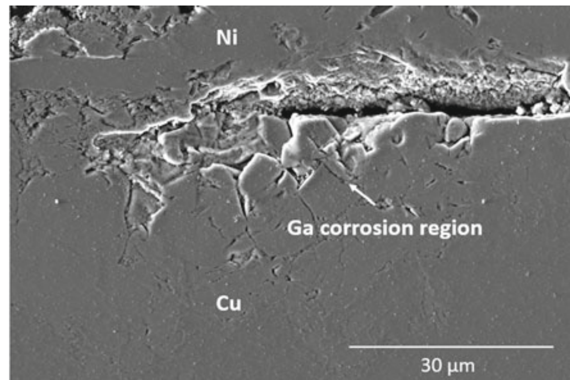

Fig. 5 Cross-section of EGaIn/Ni-Cu interface after 15 days of annealing at 125 °C showing spalling of Ni coating as a result of Ga corrosion

Ga and Ni/Cu reaction, occurring as cuboids of varying sizes. Most of the liquid metal on this sample was successfully removed through etching, revealing the underlying substrate. The interfaces of 10 days and 15 days annealed samples show similar features, as shown in Fig. 4b, c. The Ga-based liquid metal became much more difficult to remove as a result of increasing amounts of IMCs. Other than $(Ni,Cu)_3Ga_7$ cuboids, large plates of $CuGa_2$ can been seen on the surface, indicating the breach of the Ni coating by Ga. Further evidence of the breach of the Ni coating can be found in the SEM image of the cross-section of a sample annealed for 15 days. As shown in Fig. 5, after the Ni coating was breached, Ga came into contact with Cu and wet the Ni/Cu interface, causing the spalling of the Ni layer.

IMCs formed during the reflow process, as shown in Fig. 4d, e, with different morphologies than annealed samples. Colonies of large sheets of Ni_3Ga_7 along with relatively small $(Ni,Cu)_3Ga_7$ cuboids can be seen in both samples. However, further annealing at 125 °C for 5 days following the reflow process resulted in the disappearance of sheet-shaped IMCs and growth of faceted $(Ni,Cu)_3Ga_7$ prisms.

SEM images of the interface demonstrate that IMC formation between Ga and Ni is rapid at elevated temperatures. EGaIn used in this study was able to breach the 5 μm Ni coating within 10 days of annealing at 125 °C, leading to even greater extent of corrosion as Ga reacts with Cu more readily. This offers a potential explanation to the observed increase in thermal conductivity after aging. As the Ga/Ni and Ga/Cu take place, the percentage of Ga in the liquid metal TIM decreases, resulting in an enrichment of In. Since In has a higher thermal conductivity than Ga, it is thus reasonable to assume that a more In-rich alloy would show higher thermal conductivity. The decrease in thermal boundary resistance can be explained by the decrease in the Ni layer thickness and the spalling of the Ni coating.

Thermodynamics of EGaIn

Ga-based room temperature liquid metal alloys are known for their large undercooling during solidification as it is difficult for Ga to nucleate. Figure 6 shows a DSC curve of an off-eutectic Ga-In alloy. The undercooling of the alloy is measured to be 33 °C. The loop, which is also the major solidification peak, is an increase in temperature upon solidification as a result of supercooling of the liquid, known as recalescence.

DSC testing of EGaIn before and after accelerated aging on Ni-Cu substrates shows a further retardation of the onset temperature of solidification as a result of aging. As shown in Table 1, after 15 days of annealing, the onset temperature of solidification decreased by 29 °C to −47 °C, accompanied by a decrease in heat of fusion from 69.6 J/g to 31.8 J/g. Even one cycle of reflow decreases the onset

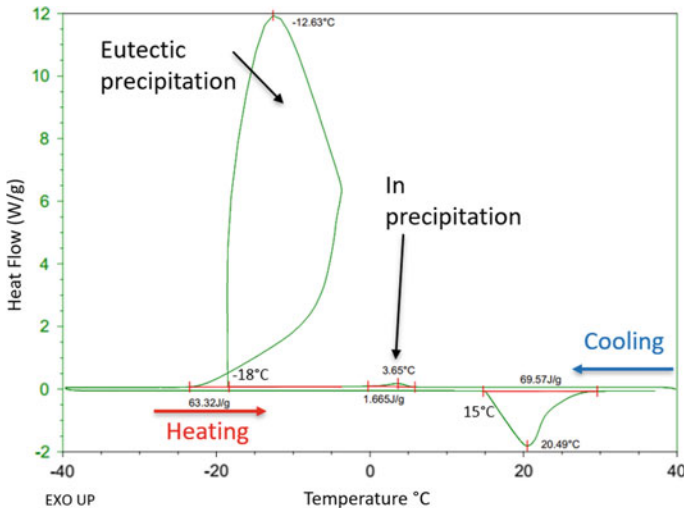

Fig. 6 DSC curve of near eutectic Ga-In alloy. Note that the equilibrium melting and solidification temperature for this alloy is 15 °C. Substantial undercooling is observed on cooling

Table 1 Summary of DSC results

	Onset temperature of solidification/°C	Heat of fusion (J/g)
Time 0	−18	69.6
5 days annealing	−28	44.4
10 days annealing	−30	32.0
15 days annealing	−47	31.8
1 × reflow	−32	67.8
5 × reflow	−32	66.4

temperature of solidification to −32 °C, while little changes to the heat of fusion are observed in reflowed samples.

Conclusion

Ga-based low melting temperature alloys are promising candidates for next generation TIMs. In this study, we focus on the direct measurement of thermal properties of EGaIn on Ni-plated Cu substrates using an IR temperature mapping setup and relate the measurements to intermetallic formation, interfacial reactions, and corrosion. Thermal property measurements confirm that Ga-based liquid metal TIM exhibits excellent thermal performance compared with conventional TIMs. Counterintuitively, an increase in thermal conductivity and a decrease in thermal boundary resistance were observed after accelerated aging either by annealing at 125 °C or reflowing.

Interfacial reaction study using SEM shows rapid IMC formation between Ga and Ni at elevated temperatures. The 5-micron Ni coating on the Cu substrate was breached within 10 days of annealing at 125 °C, leading to spalling of the Ni layer. The enrichment of In in the liquid metal system as a result of Ga consumption is the likeliest explanation for the observed increase in thermal conductivity after aging. At the same time, the decrease in Ni layer thickness and direct contact between Cu and Ga explain the decreased contact resistance as a result of aging. The rapid interfacial reaction observed in this study also suggests the necessity of a protective layer to be used on metal substrates in the presence of Ga-based TIMs.

Acknowledgements Research funding from Purdue University's Cooling Technologies Research Center (CTRC), an industry-funded, graduated National Science Foundation Industry/University Cooperative Research Center, is gratefully acknowledged. Alsaati acknowledges the support of a Saudi Arabia Cultural Mission (SACM) fellowship, sponsored by the Saudi Arabian Ministry of Education.

References

1. Gwinn JP, Webb RL (2003) Performance and testing of thermal interface materials. Microelectron J 34(3):215–222
2. Yu W et al (2015) Exceptionally high thermal conductivity of thermal grease: synergistic effects of graphene and alumina. Int J Therm Sci 91:76–82
3. Duggin MJ (1969) The thermal conductivity of liquid gallium. Phys Lett A 29(8):470–471
4. Roy CK et al (2015) Investigation into the application of low melting temperature alloys as wet thermal interface materials. Int J Heat Mass Transf 85:996–1002
5. Dickey MD et al (2008) Eutectic gallium-indium (EGaIn): a liquid metal alloy for the formation of stable structures in microchannels at room temperature. Adv Funct Mater 18(7):1097–1104

6. Cochran CN, Foster LM (1962) Vapor pressure of gallium, stability of gallium suboxide vapor, and equilibria of some reactions producing gallium suboxide vapor. J Electrochem Soc 109(2):144
7. Hardy SC (1985) The surface tension of liquid gallium. J Cryst Growth 71(3):602–606
8. Kolman DG (2019) A review of recent advances in the understanding of liquid metal embrittlement. Corrosion 75(1):42–57
9. Deng Y-G, Liu J (2009) Corrosion development between liquid gallium and four typical metal substrates used in chip cooling device. Appl Phys A 95(3):907–915
10. Doudrick K et al (2014) Different shades of oxide: from nanoscale wetting mechanisms to contact printing of gallium-based liquid metals. Langmuir 30(23):6867–6877
11. Tang J et al (2017) Gallium-based liquid metal amalgams: transitional-state metallic mixtures (TransM2ixes) with enhanced and tunable electrical, thermal, and mechanical properties. ACS Appl Mater interfaces 9(41):35977–35987
12. Mei S et al (2014) Thermally conductive and highly electrically resistive grease through homogeneously dispersing liquid metal droplets inside methyl silicone oil. J Electron Packaging 136(1):011009
13. Wang X et al (2018) Soft and moldable Mg-Doped liquid metal for conformable skin tumor photothermal therapy. Adv Healthc Mater 7(14):1800318
14. Kong W et al (2019) Oxide-mediated formation of chemically stable tungsten–liquid metal mixtures for enhanced thermal interfaces. Adv Mater 31(44):1904309
15. Chang H et al (2020) Recoverable liquid metal paste with reversible rheological characteristic for electronics printing. ACS Appl Mater Interfaces 12(12):14125–14135
16. Wei S et al (2019) Investigation on enhancing the thermal conductance of gallium-based thermal interface materials using chromium-coated diamond particles. J Mater Sci Mater Electron 30(7):7194–7202
17. Gao Y et al (2017) Investigation on the optimized binary and ternary gallium alloy as thermal interface materials. J Electron Packaging 139(1):011002
18. Uppal A et al (2019) Pressure-activated thermal transport via oxide shell rupture in liquid metal capsule beds. ACS Appl Mater Interfaces 12(2):2625–2633
19. Tutika R et al (2018) Mechanical and functional tradeoffs in multiphase liquid metal, solid particle soft composites. Adv Funct Mater 28(45):1804336
20. Gaitonde A, Nimmagadda A, Marconnet A (2017) Measurement of interfacial thermal conductance in Lithium ion batteries. J Power Sources 343:431–436
21. Marconnet AM et al (2011) Thermal conduction in aligned carbon nanotube–polymer nanocomposites with high packing density. ACS Nano 5(6):4818–4825